Electrical Power and Energy Systems 65 (2015) 220–230

Contents lists available at ScienceDirect

Electrical Power and Energy Systems

journal homepage: www.elsevier.com/locate/ijepes

Effective oscillation damping of an interconnected multi-source power system with automatic generation control and TCSC

Kazem Zare *, Mehrdad Tarafdar Hagh, Javad Morsali

Faculty of Electrical and Computer Engineering, University of Tabriz, Tabriz, Iran

ARTICLE INFO

Article history:
Received 23 October 2013
Received in revised form 29 August 2014
Accepted 12 October 2014

Keywords:
AGC
TCSC
Oscillation damping
IPSO
Stability enhancement

ABSTRACT

Stabilizing area frequency and tie-line power oscillations in interconnected power systems are main concerns that have received significant attention in automatic generation control (AGC) studies. This paper deals with modeling and simulation of thyristor controlled series capacitor (TCSC) based damping controller in coordination with AGC to damp the oscillations and thereby, improve the dynamic stability. The contribution of TCSC in tie-line power exchange is formulated analytically for small perturbation and a systematic method based on the Taylor series expansion is proposed for modeling of TCSC based damping controller. The integral gains of AGC and TCSC parameters are optimized simultaneously using an improved particle swarm optimization (IPSO) algorithm through minimizing integral of time multiplied squared error (ITSE) performance index. The performance of the proposed TCSC–AGC coordinated controller is compared with case of AGC alone. A two-area interconnected multi-source power system, including TCSC located in series with the tie-line, is studied considering nonlinearity effects of generation rate constraint (GRC) and governor dead band (GDB). Simulation results show that proposed controller shows greater performance in damping of the oscillations and enhancing the frequency stability. Furthermore, sensitivity analyses are carried out against system loading condition, parametric uncertainties, and different perturbation patterns to show the robustness of TCSC–AGC.

Introduction

Review on AGC in the presence of FACTS

Studying automatic generation control (AGC) of power system in presence of flexible ac transmission system (FACTS) devices is an interesting topic that has received much attention in literature. Various FACTS controllers can be applied in series with tie-line of interconnected power systems to control power flow and to damp the inter-area oscillations via designing a supplementary controller. Due to quick dynamic responses, series FACTS devices such as thyristor controlled phase shifter (TCPS) [1–8], static synchronous series compensator (SSSC) [7,9], and interline power flow controller (IPFC) [10,11] have been employed in power system to attenuate the area frequency and tie-line power oscillations. Energy storage devices based on FACTS such as superconducting magnetic energy storage (SMES) [2,3,5,7], capacitive energy storage (CES) [1], and redox flow batteries (RFB) [6,10,11] can compensate the sudden load perturbations by injecting or absorbing the active power to the system and thereby stabilize the oscillations. Authors in [1] present comparative performance evaluation of TCPS and CES for AGC of an interconnected two-area power system. In [2], AGC of a two-area interconnected non-reheat thermal-thermal power system is studied with and without coordinated control of SMES and TCPS. In [3], to improve the dynamic performance of AGC of an interconnected hydro-thermal power system, coordinated design of SMES and TCPS is proposed. In [4], the analysis of AGC of a two-area interconnected power system under open market scenario in the presence of TCPS is investigated. Authors in [5] deal with the coordinated design of TCPS and SMES in corporation with dynamic active power support from wind farm for frequency control of a two-area power system in deregulated environment. In [6], decentralized controllers are designed for LFC of interconnected reheat thermal-thermal power system with and without RFB and TCPS in the tie-line. A comparative study on evaluating the dynamic performance of coordinated designs of SMES–SMES, TCPS–SMES and SSSC–SMES controllers with AGC of an interconnected hydro–hydro power system is carried out in [7]. In [8], load frequency control (LFC) of a two-area multi-source power system including TCPS in series with tie-line is studied to enhance the dynamic performance. In [9], AGC study of a two-area hydro-thermal power system is performed under

* Corresponding author. Tel./fax: +98 411 3300829.
E-mail addresses: kazem.zare@tabrizu.ac.ir (K. Zare), tarafdar@tabrizu.ac.ir (M.T. Hagh), morsali@tabrizu.ac.ir (J. Morsali).

http://dx.doi.org/10.1016/j.ijepes.2014.10.009
0142-0615/

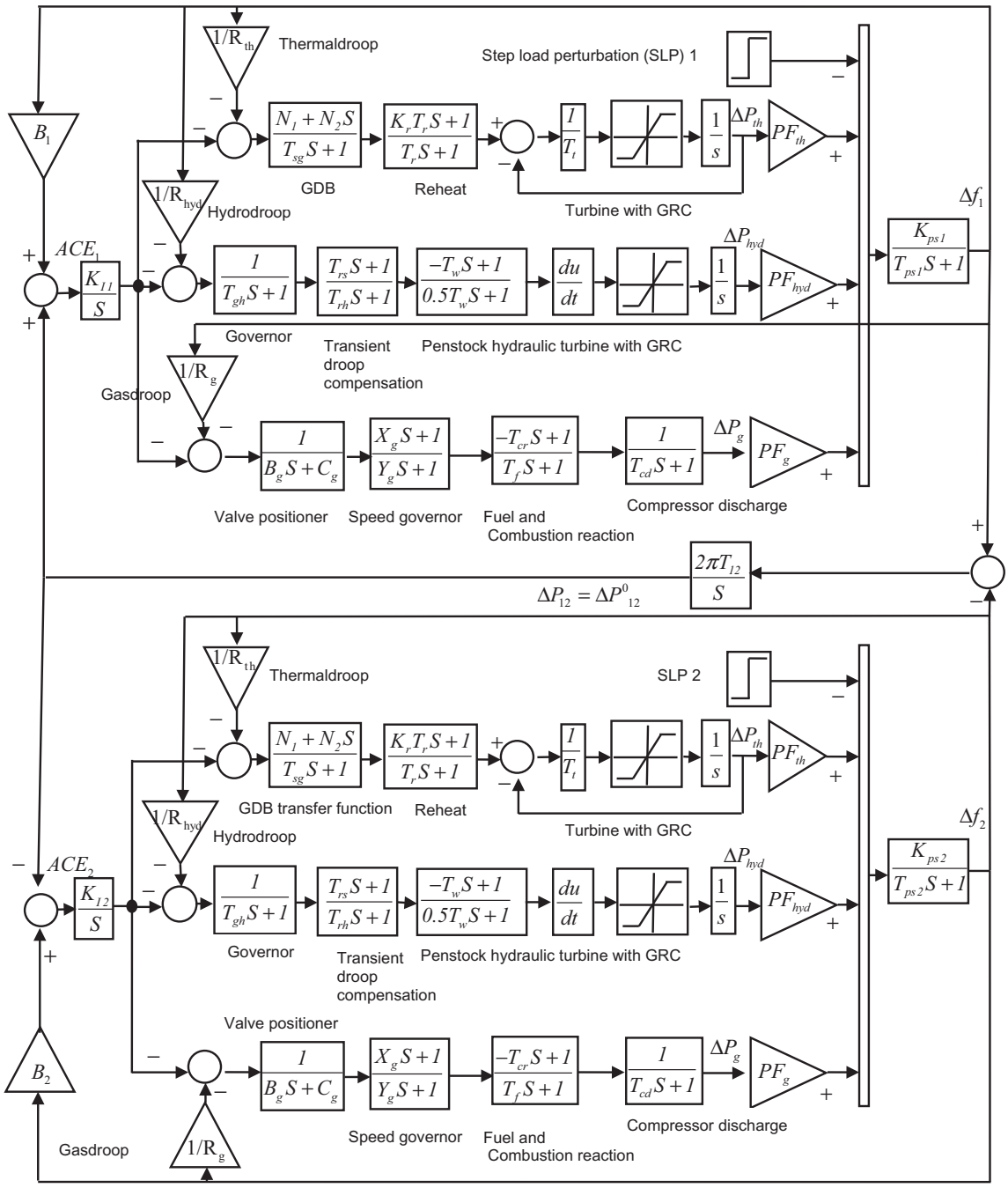

Fig. 1. Transfer function model of proposed multi-source power system considering GRC and GDB.

Table 1
Parameters description of the interconnected multi-source power system.

R_{th}, R_{hyd}, and R_g	Governor speed regulation parameters of thermal, hydro and gas units	PF_{th}, PF_g and PF_{hyd}	Participation factors of thermal, gas, and hydro units
T_{sg}	Governor time constant of steam turbine	B_g	Time constant of the valve positioner
T_t	Steam turbine time constant	T_{gh}	Hydro turbine governor time constant
T_w	Starting time of water in hydro turbine	T_{cd}	Compressor discharge volume time constant
K_r	Steam turbine reheat constant	C_g	Gas turbine valve positioner
T_r	Steam turbine reheat time constant	T_f	Gas turbine fuel time constant
T_{ps1}, T_{ps2}	Power system time constants	T_{cr}	Gas turbine combustion reaction time delay
K_{ps1}, K_{ps2}	Power system gains	T_{rs}	Hydro turbine speed governor reset time
X_g	Lead time constant of gas turbine governor	T_{12}	Synchronizing coefficient
Y_g	Lag time constant of gas turbine governor	B_1, B_2	Frequency bias coefficients

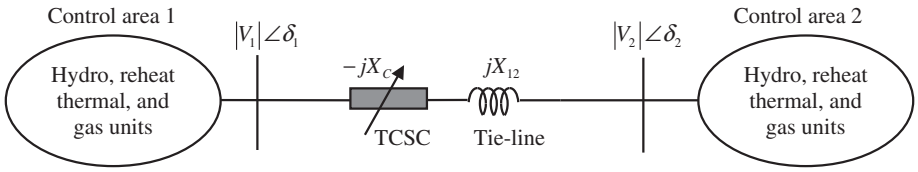

Fig. 2. Two-area interconnected hydro, thermal, gas power system with TCSC in series with the tie-line.

deregulated environment. The dynamic performance of SSSC is compared with the TCPS in terms of settling time and overshoot to reduce area frequency tie line power deviations. The coordinated design of redox flow batteries (RFB) and interline power flow controller (IPFC) is studied in [10,11] to enhance LFC of a multi-source interconnected power system in order to stabilize the area frequency and tie-line power oscillations. Thyristor controlled series capacitor (TCSC) as a high-performance and cost-effective series FACTS can be used in power systems as series compensator for fine and secured optimal power flow control in transmission lines [12,13]. The series compensation by TCSC is one of the most economic ways to increase the capability of the line power transfer [14,15]. TCSC controller can be used to mitigate effectively the sub-synchronous resonance (SSR) [14]. Additionally, a supplementary power oscillation damping (POD) controller can be applied to improve the rotor angle stability [14,16,17]. Simultaneous coordinated design of TCSC-based POD controller and power system stabilizer (PSS) are studied widely in the literature to improve the rotor angle stability of power systems [18–20]. Simple and fast implementation and adjustment of the lead-lag controllers cause the engineers prefer these linear structures in power system applications, so far [13,21]. Since one of main power system issues is the AGC in the presence of FACTS devices, the modeling and simulation of TCSC are major gaps and need further investigations. To the best of authors' knowledge, no significant work has been reported in literature to study the effect of TCSC in AGC problem of an interconnected power system, till now. It is possible to decrease the area frequency and tie-line power oscillations by dynamic controlling series impedance of the tie-line with TCSC. For the first time, modeling and simulation of TCSC which are applicable in AGC studies are investigated in current paper.

Review on realistic considerations in AGC performance evaluation

In order to get a precise realization of the AGC issue, it is important to take into account the main intrinsic requirements such as physical constraints of generation rate constraint (GRC) and governor dead-band (GDB) nonlinearities [22,23]. The review of literature on AGC in the presence of FACTS devices reveals that in most of papers [5–11], GRC and GDB nonlinearities of hydro and thermal units are not considered. It is found that evaluating the AGC performance without considering aforementioned constraints and multi-source power generation in each control area, may not represent realistic performance of FACTS and AGC in power system dynamics [24]. Ref. [25] deals with studying the performance of AGC in a two-area power system comprising thermal, hydro, and gas units working together in each area. However, the share of each generator in total generation of the area, and also the GRC and GDB effects are not considered. In [26,27], AGC of multi-source power system, which has thermal, hydro, and gas generation units, is studied in which the contribution of each unit in total generation is represented by a participation factor. However, it is supposed that only thermal and gas units take part in AGC of the system and the hydro plant is uncontrolled. Similarly, the nonlinearity effects of GRC and GDB are not considered. In [28], the LFC of a single-area power system with diverse power generations is presented by optimal output feedback approach in which the suitable GRC is considered for thermal and hydro units. In [8], LFC of a two-area multi-source power system which has various generations from reheat thermal, gas, and hydro units with a TCPS in series with the tie-line is presented. In [29], LFC of a single-area multi-source power system is studied which contains the reheat thermal, hydro and gas power plants. Then, a two-area multi-source power system based on [8] is proposed in which a HVDC link is also considered in parallel with existing AC tie-line to interconnect the two areas. However, the nonlinearity effect of GRC of thermal and hydro units and the deteriorating effect of GDB in thermal unit are not considered in [8,29]. Surprisingly, literature survey shows that no effort has been made to evaluate the dynamic performance of AGC in a realistic multi-source power system with gas, reheat thermal, and hydro units considering GRC and GDB nonlinearities all together even without FACTS.

Main contributions of this study

In this paper for the first time, TCSC is employed in coordination with AGC of a realistic interconnected multi-source power system to damp effectively tie-line power and area frequency oscillations. The integral gains of AGC and adjustable parameters of TCSC are optimized by an improved particle swarm optimization (IPSO) algorithm. Regarding above survey, the main contributions of this paper are:

(a) Extraction of incremental tie-line power flow model considering TCSC application in AGC studies.
(b) Proposing a novel modeling method based on the Taylor series expansion for TCSC based damping controller.
(c) Validating the dynamic performance of TCSC–AGC coordinated controller on a realistic interconnected multi-source power system which contains the gas, hydro, and reheat thermal units considering GRC and GDB nonlinearities.
(d) Performing robustness analysis against uncertainties in parameters and loading condition.
(e) Analysing the impact of different load perturbation patterns on the dynamic performance of proposed TCSC–AGC controller.
(f) Proposing an advanced TCSC based damping controller in addition to the basic model.

Investigated power system and dynamic modeling of TCSC

Realistic interconnected multi-source power system

The investigated system is a two-area interconnected multi-source power system with reheat thermal, hydro, and gas units in each control area. Fig. 1 shows the transfer function model of proposed realistic power system. The block descriptions of hydro, reheat thermal, and gas plants are shown on Fig. 1. All power plants in each area are lumped together to make a control area which is represented by an equivalent plant dynamics.

Appropriate GRC models for the hydro and thermal units and GDB for the thermal units in both areas are considered. Parameters

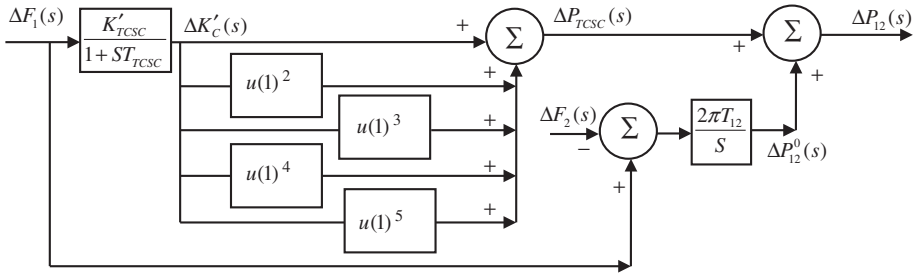

Fig. 3. Basic structure for the proposed TCSC-based damping controller.

of the multi-source system are described in Table 1 and are given in [8]. The GDB is defined as the total magnitude of a sustained speed change within which there is no change in valve position of the turbine. The GDB of the backlash type can be linearized in terms of change and the rate of change in the speed. In this paper, following most recent papers [21,30], the Fourier coefficients of N_1 and N_2 in the GDB transfer function model are $N_1 = 0.8$ and $N_2 = -0.2/\pi$, respectively. In practice, the rate of active power change, which can be achieved by thermal and hydro units, has a maximum limit [31]. So, the designed LFC for the unconstrained generation rate situation may not be suitable and realistic. The appropriate GRC of 10% per minute for thermal unit of Fig. 1 is considered for both raising and falling rates. For the hydro unit, typical GRC of 270% per minute for raising generation and 360% per minute for falling generation are considered [1,3,28].

Incremental tie-line power flow model considering TCSC applicable for AGC

When a TCSC is placed in series with the tie-line as shown in Fig. 2, the tie-line power flow can be expressed as [32,33]:

$$P_{12} = \frac{|V_1| \cdot |V_2|}{X_{12} - X_C} \sin(\delta_1 - \delta_2) \tag{1}$$

where X_{12} is the tie-line reactance, X_c is the TCSC reactance connected in series with the tie-line, δ_1 and δ_2 are the voltage angles of area 1 and area 2, respectively.

Considering the series compensation ratio of $K_C = X_C/X_{12}$, (1) can be rewritten as [32,33]:

$$P_{12} = \frac{|V_1| \cdot |V_2|}{X_{12}(1 - K_C)} \sin(\delta_1 - \delta_2) \tag{2}$$

Eq. (2) can be divided into two terms as:

$$P_{12} = \frac{|V_1| \cdot |V_2|}{X_{12}} \sin(\delta_1 - \delta_2) + \frac{K_C}{1 - K_C} \cdot \frac{|V_1| \cdot |V_2|}{X_{12}} \sin(\delta_1 - \delta_2) \tag{3}$$

The first term in (3) explains the power flow in tie-line without the TCSC, and the second term in (3) depicts effect of presence of the TCSC in tie-line power flow. For small perturbation in δ_1, δ_2, and K_C from their nominal values δ_1^0, δ_2^0, by taking into account the idea discussed in [2–5,7] about linearizing around an operating point, the incremental tie-line power flow can be obtained as:

$$\Delta P_{12} = \frac{|V_1| \cdot |V_2|}{X_{12}} \cos(\delta_1^0 - \delta_2^0) \sin(\Delta\delta_1 - \Delta\delta_2) + \frac{\Delta K_C}{1 - \Delta K_C} \cdot \frac{|V_1| \cdot |V_2|}{X_{12}} \sin(\delta_1^0 - \delta_2^0) \tag{4}$$

Table 2
Adjustable parameters of controllers.

Controller	Adjustable parameters
Integral controller (just AGC)	K_{I1}, K_{I2}
TCSC–AGC coordinated controller	T_{TCSC}, K_{TCSC}, K_{I1}, K_{I2}

Since for a small change in real power load, the variation of bus voltage angles is practically very small [2,4,5,7], it is reasonable to assume that $\sin(\Delta\delta_1 - \Delta\delta_2) \approx \Delta\delta_1 - \Delta\delta_2$. Therefore,

$$\Delta P_{12} = \frac{|V_1| \cdot |V_2|}{X_{12}} \cos(\delta_1^0 - \delta_2^0)(\Delta\delta_1 - \Delta\delta_2) + \frac{\Delta K_C}{1 - \Delta K_C} \cdot \frac{|V_1| \cdot |V_2|}{X_{12}} \sin(\delta_1^0 - \delta_2^0) \tag{5}$$

Let's denote $T_{12} = \frac{|V_1| \cdot |V_2|}{X_{12}} \cos(\delta_1^0 - \delta_2^0)$ and $K_1 = \frac{|V_1| \cdot |V_2|}{X_{12}} \sin(\delta_1^0 - \delta_2^0)$

Thus, (5) reduces to:

$$\Delta P_{12} = T_{12}(\Delta\delta_1 - \Delta\delta_2) + \frac{\Delta K_C}{1 - \Delta K_C} \cdot K_1 \tag{6}$$

As $\Delta\delta_1 = 2\pi \int \Delta f_1 dt$ and $\Delta\delta_2 = 2\pi \int \Delta f_2 dt$ [3,4], Laplace transform of (6) can be written as:

$$\Delta P_{12}(s) = \frac{2\pi T_{12}}{S}[\Delta F_1(s) - \Delta F_2(s)] + \frac{\Delta K_C}{1 - \Delta K_C} \cdot K_1 \tag{7}$$

From the Taylor series expansion method, we know that for $|x| < 1$:

$$\frac{1}{1 - x} = 1 + x + x^2 + x^3 + x^4 + \ldots \tag{8}$$

Since in the series compensation with the TCSC, the compensation ratio is bounded to the range $(-1, 1)$ i.e., $|\Delta K_C| < 1$ for both capacitive and inductive operation modes, we can employ the Taylor series expansion in (8) to the modeling of the TCSC controller as:

$$\frac{\Delta K_C}{1 - \Delta K_C} = \Delta K_C + \Delta K_C^2 + \Delta K_C^3 + \Delta K_C^4 + \Delta K_C^5 + \ldots \tag{9}$$

Therefore, (7) can be rewritten as:

$$\Delta P_{12}(s) = \Delta P_{12}^0(s) + (\Delta K_C + \Delta K_C^2 + \Delta K_C^3 + \Delta K_C^4 + \Delta K_C^5 + \ldots)K_1 \tag{10}$$

where ΔP_{12}^0 denotes the tie-line power flow exchange without TCSC as:

$$\Delta P_{12}^0(s) = \frac{2\pi T_{12}}{S}[\Delta F_1(s) - \Delta F_2(s)] \tag{11}$$

As it is obvious in (10), the tie-line power flow exchange can be regulated by controlling the compensation ratio ΔK_C. In this paper, ΔK_C is introduced as:

$$\Delta K_C(s) = \frac{K_{TCSC}}{1 + ST_{TCSC}} \Delta Error(s) \tag{12}$$

The basic structure of proposed TCSC-based controller is depicted in Fig. 3 where the frequency deviation in area 1 i.e., Δf_1 is used as the control signal to the TCSC ($\Delta Error(s) = \Delta F_1(s)$).

Table 3
Some near optimal adjusted parameters of the controllers.

		K_{I1}	K_{I2}	K_{TCSC}	T_{TCSC}	ITSE index
Only AGC	1	0.0851	0.0478	–	–	0.0621
	2	0.0851	0.0427	–	–	0.0622
	3	0.0850	0.0424	–	–	0.0622
	4	0.0791	0.0524	–	–	0.0622
	5	*0.0851*	*0.0457*	–	–	*0.0621*
TCSC–AGC	1	0.1176	0.1692	0.1812	0.0060	0.0255
	2	*0.1177*	*0.1680*	*0.2093*	*0.0037*	*0.0255*
	3	0.1174	0.1551	0.1938	0.0047	0.0255
	4	0.1202	0.1606	0.2310	0.0033	0.0256
	5	0.1183	0.1620	0.2572	0.0038	0.0257

It should be noted that according to the design objectives, only the first five terms in (10) are used in Fig. 3. The accuracy of this approximation is high and enough to avoid unnecessary and excessive complexities of simulations. The constant of K_1 is included in the TCSC gain K_{TCSC} i.e., $K'_{TCSC} = K_{TCSC} \cdot K_1$ the signal of $u(1)$ in Fig. 3 denotes the value of $\Delta K_C(s)$ signal. Thus, in the presence of TCSC controller, the tie-line power deviation model of Fig. 1 should be modified by the proposed model depicted in Fig. 3 in which:

$$\Delta P_{TCSC} = \Delta K'_C + \Delta K'^2_C + \Delta K'^3_C + \Delta K'^4_C + \Delta K'^5_C \tag{13}$$

where

$$\Delta K'_C(s) = \frac{K'_{TCSC}}{1 + ST_{TCSC}} \Delta F_1(s) \tag{14}$$

Actually, Taylor series expansion is a representation of a real or complex-valued function as sum of infinitely differentiable terms that are calculated on an open interval from the values of the function's derivatives at a real or complex number [34]. It is routine practice to approximate the value of a function by considering a finite number of terms of its Taylor series. Any finite number of initial terms of the Taylor series of a function is called a Taylor polynomial. The partial sums (the Taylor polynomials) of the series can be used as approximations of the entire function. Taylor's theorem provides quantitative estimates on the error of approximation which can be negligible if enough terms are comprised. The proposed TCSC control method based on Taylor polynomials is analytical, simple to follow, easy to implement in MATLAB/Simulink environment, and flexible to change its order of approximation.

Objective function and its solution

Objective function for controller design

In order to effectively damping the oscillations, considering a suitable objective function is very important to find the controller parameters. In this paper, the integral of time multiplied squared

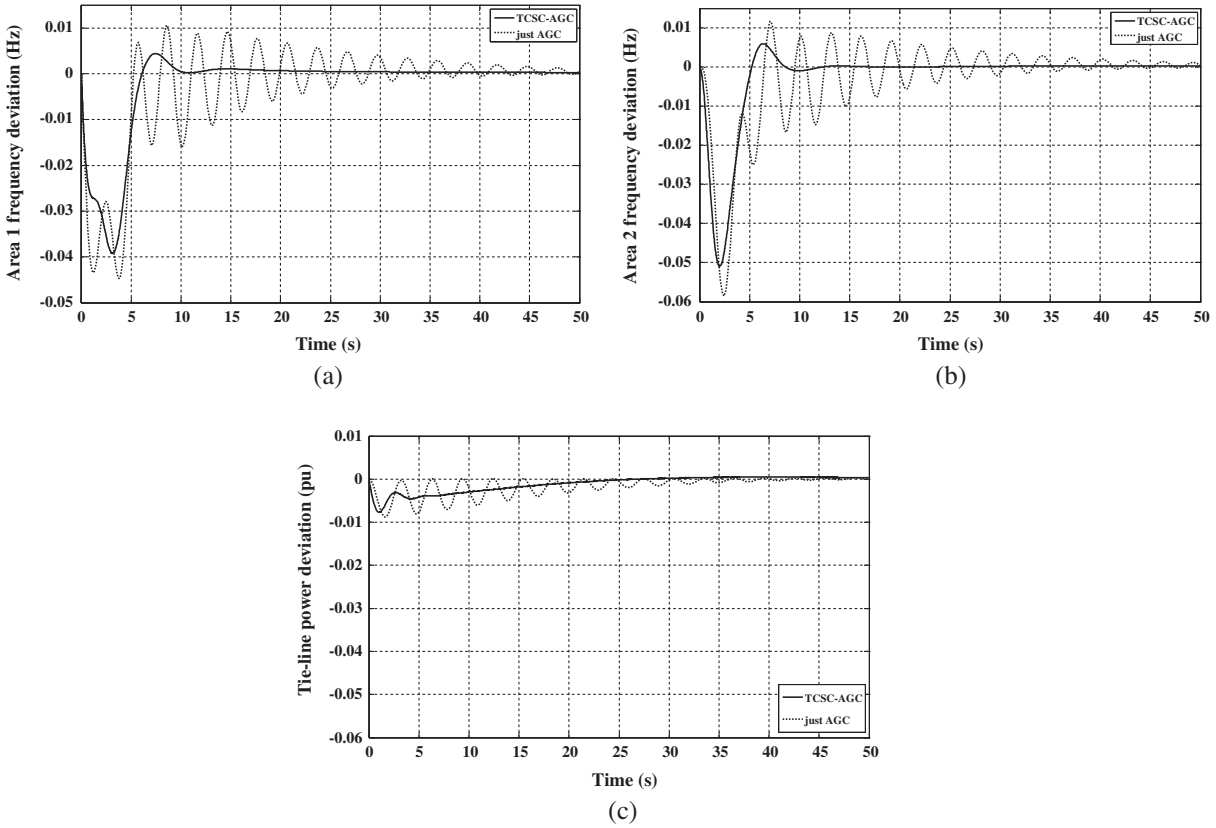

Fig. 4. Dynamic responses to the 0.01 P.U. SLP in area 1, (a) area 1 frequency deviation Δf_1, (b) area 2 frequency deviation Δf_2, and (c) tie-line power deviation ΔP_{12}.

Table 4
System damping characteristics with the optimized controllers.

	System oscillatory modes	ζ	Signal	M_p	T_P	T_S
Just AGC	−0.1711 ± 2.0357i	0.0837	Δf_1	0.0448	3.7452	48.4881
	−0.6231 ± 0.5778i	0.7333	Δf_2	0.0585	2.4691	50
	−0.0695 ± 0.0251i	0.9407	ΔP_{12}	0.0088	1.6309	38.2690
TCSC−−AGC	−0.8961 ± 1.9579i	0.4162	Δf_1	0.0392	3.1305	25.2906
	−0.5500 ± 0.5660i	0.6969	Δf_2	0.0510	2.0202	11.2258
	−0.0680 ± 0.0584i	0.7587	ΔP_{12}	0.0077	1.0006	22.5292

error (ITSE) performance index is considered as the objective function as following:

$$ITSE = \int_0^{T_{sim}} t[\Delta f_1^2 + \Delta f_2^2 + \Delta P_{12}^2]dt \quad (15)$$

where T_{sim} denotes the simulation time. The ITSE index uses advantages of both integral of squared error (ISE) and integral of time multiplied absolute error (ITAE) indices, as it utilizes squared error and time multiplication to weight large oscillations and penalize long settling time. The ITSE performance index has been employed recently in [21,30,35] to design AGC of interconnected power systems. Table 2 shows the adjustable parameters of the considered controllers in this paper.

An optimization problem is solved by an improved particle swarm optimization (IPSO) algorithm to minimize the ITSE index to obtain the optimal parameters of the controllers, subject to following constraints:

$$\begin{aligned} K_{I1}^{\min} &\leqslant K_{I1} \leqslant K_{I1}^{\max} \\ K_{I2}^{\min} &\leqslant K_{I2} \leqslant K_{I2}^{\max} \\ K_{TCSC}^{\min} &\leqslant K_{TCSC} \leqslant K_{TCSC}^{\max} \\ T_{TCSC}^{\min} &\leqslant T_{TCSC} \leqslant T_{TCSC}^{\max} \end{aligned} \quad (16)$$

where the minimum and maximum values of parameters are chosen as 0 and 2, respectively.

IPSO algorithm

PSO is a member of wide category of swarm intelligence-based optimization algorithms. PSO is one of most well-known heuristic evolutionary algorithms which have found many applications in solving of engineering optimization problems. In the case of populations with large diversity, an improved PSO (IPSO) algorithm recently has been introduced in [36], which employs crossover operator so that the search space can be successfully surveyed. This contributes in finding the global optimal solution more precisely. IPSO is employed here to minimize the ITSE objective function due to its convergence effectiveness in optimizing the parameters. To find the optimal control parameters, the IPSO should explore in multi-dimensional search space. To start optimization process, initially some executions are performed with different values of the IPSO parameters to assess whether IPSO will find satisfactory results or not. The parameters of IPSO algorithm should be selected carefully to provide high performance. For our provided MATLAB-based IPSO program, these parameters are chosen as: $n = 30$; $m = 6$; $\omega_{min} = 0.4$; $\omega_{max} = 0.9$; $c_1 = c_2 = 2$; $\gamma = 0.1$; $t_{max} = 30$; and

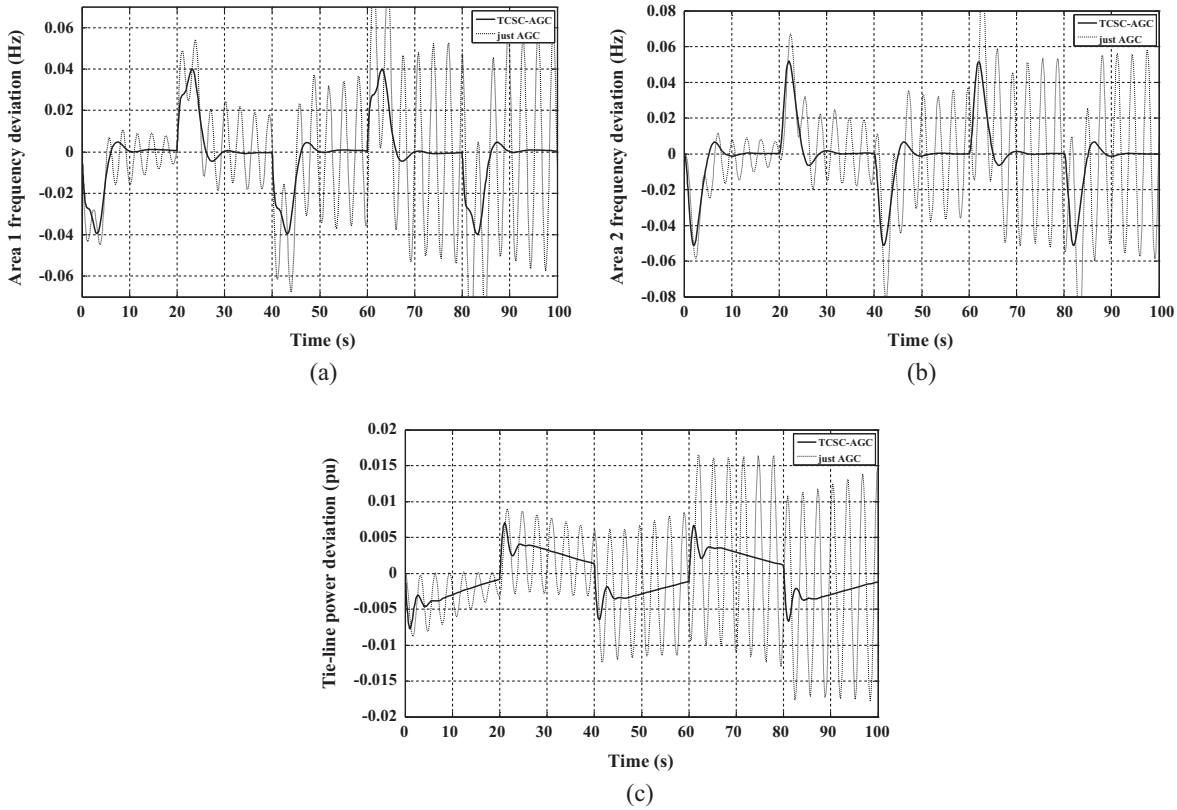

Fig. 5. Dynamic responses to the pulse load perturbation in area 1: (a) area 1 frequency deviation, (b) area 2 frequency deviation, and (c) tie-line power deviation.

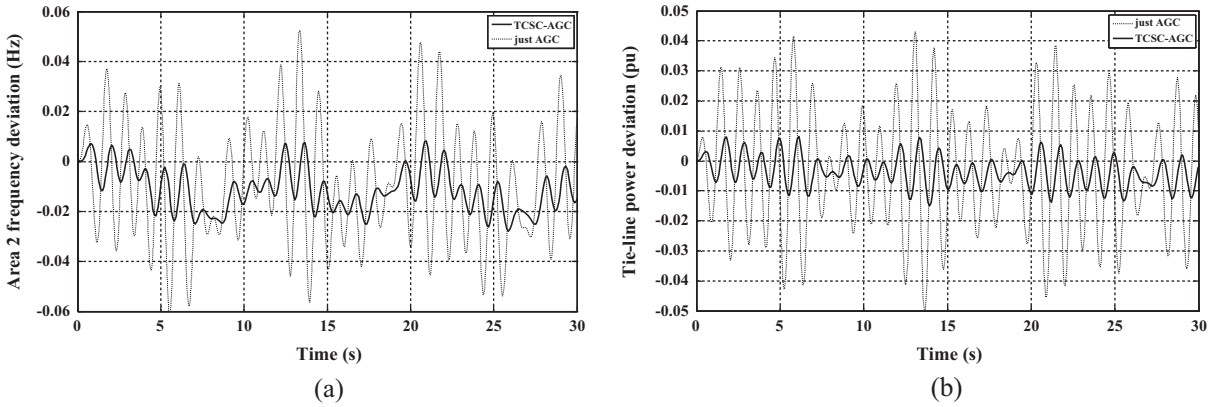

Fig. 6. Dynamic responses to the sinusoidal load perturbation, (a) area 2 frequency deviation, and (b) tie-line power deviation.

CR = 0.6, where n is the population size; m is total number of parameters to be optimized; ω_{max}, ω_{min} are the initial and final inertia weights; c_1, c_2 are acceleration coefficients; γ is a chosen number in interval (0, 1) to control the maximum velocity vector; t_{max} is total number of the iterations; and CR is crossover rate.

Simulation results and discusses

Simulation procedure

Before explanation of the simulation results, it is helpful to list briefly what simulation procedure we are going to perform in continue of this paper to demonstrate the effectiveness of our proposed method. The simulation procedure can be divided into following subsections:

- Performance evaluation of the proposed basic method of TCSC modeling under step load perturbation (SLP) in area 1.
- Further performance analyses for different load perturbation patterns:
  (1) Pulse load perturbation.
  (2) Sinusoidal load perturbation.
- Sensitivity analysis to evaluate the robustness of the proposed method against ±50% uncertainty in system loading condition and parametric uncertainties.
- Comparison between proposed advanced and basic methods for modeling of TCSC.

The simulation results are obtained by MATLAB 7.8.0 (R2009a) software on a laptop with an Intel Core™ 2 Duo of 2.66 GHz, 4 GB DDR3 RAM. The dynamic model of the investigated power system has been developed in the MATLAB/SIMULINK environment and the IPSO program has been coded as .m file to solve the optimization problem.

Simulation of the realistic power system for step load perturbation (SLP)

In this case, the time domain simulations are realized for 0.01 P.U. step load perturbation (SLP) in area 1 considering the GRC and GDB nonlinearity effects. The proposed IPSO algorithm is repeated many times to solve the optimization problem. Some near optimal solutions for nominal system parameters obtained after numerous runs are shown in Table 3. The solution with minimum value of the ITSE index is chosen as final optimized parameters of the controller which is highlighted in Table 3.

It is clear from Table 3 that with only AGC, the value of ITSE index (0.0621) is more than two times larger than the corresponding value with AGC–TCSC controller (0.0255) which means greater performance of proposed controller. Fig. 4 depicts the frequencies and tie-line power oscillation responses.

In order to show the effectiveness of the proposed TCSC–AGC coordinated controller, the responses are compared with those obtained with the case of just AGC scenario. The damping criteria such as maximum peak (M_p), peak time (T_P), and settling time

Table 5
System damping characteristics with TCSC–AGC controller considering various uncertainty scenarios.

Uncertainty	Case	% Change	Oscillatory modes	ζ	ITSE	Signal	M_p	T_P	T_S
Loading condition	Case 1	+50	−0.9237 ± 1.9518i	0.4278	0.0220	Δf_1	0.0366	3.0832	26.5109
			−0.5903 ± 0.5771i	0.7151		Δf_2	0.0484	1.9874	11.0408
			−0.0680 ± 0.0583i	0.7590		ΔP_{12}	0.0076	1.0006	22.6527
	Case 2	−50	−0.8688 ± 1.9638i	0.4046	0.0304	Δf_1	0.0422	3.1800	23.9952
			−0.5080 ± 0.5549i	0.6753		Δf_2	0.0538	2.0483	11.6564
			−0.0680 ± 0.0584i	0.7585		ΔP_{12}	0.0078	1.0006	22.5292
T_{sg}	Case 3	+50	−0.8857 ± 1.9712i	0.4099	0.0258	Δf_1	0.0394	3.1305	25.2154
			−0.5477 ± 0.5742i	0.6902		Δf_2	0.0512	2.0202	11.2731
			−0.0679 ± 0.0585i	0.7579		ΔP_{12}	0.0077	1.0006	22.5292
	Case 4	−50	−0.9040 ± 1.9437i	0.4217	0.0251	Δf_1	0.0390	3.1198	25.3510
			−0.5519 ± 0.5581i	0.7031		Δf_2	0.0507	2.0095	11.1998
			−0.0681 ± 0.0583i	0.7596		ΔP_{12}	0.0077	1.0006	22.5412
T_{12}	Case 5	+50	−0.8176 ± 2.3780i	0.3251	0.0247	Δf_1	0.0422	2.8620	22.1303
			−0.5494 ± 0.5619i	0.6991		Δf_2	0.0485	1.8483	10.8823
			−0.0683 ± 0.0591i	0.7559		ΔP_{12}	0.0079	0.9379	40.8832
	Case 6	−50	−1.0820 ± 1.3702i	0.6197	0.0279	Δf_1	0.0327	3.4171	32.2348
			−0.5450 ± 0.5799i	0.6849		Δf_2	0.0535	2.2333	11.8414
			−0.0673 ± 0.0561i	0.7683		ΔP_{12}	0.0075	1.1857	23.2079

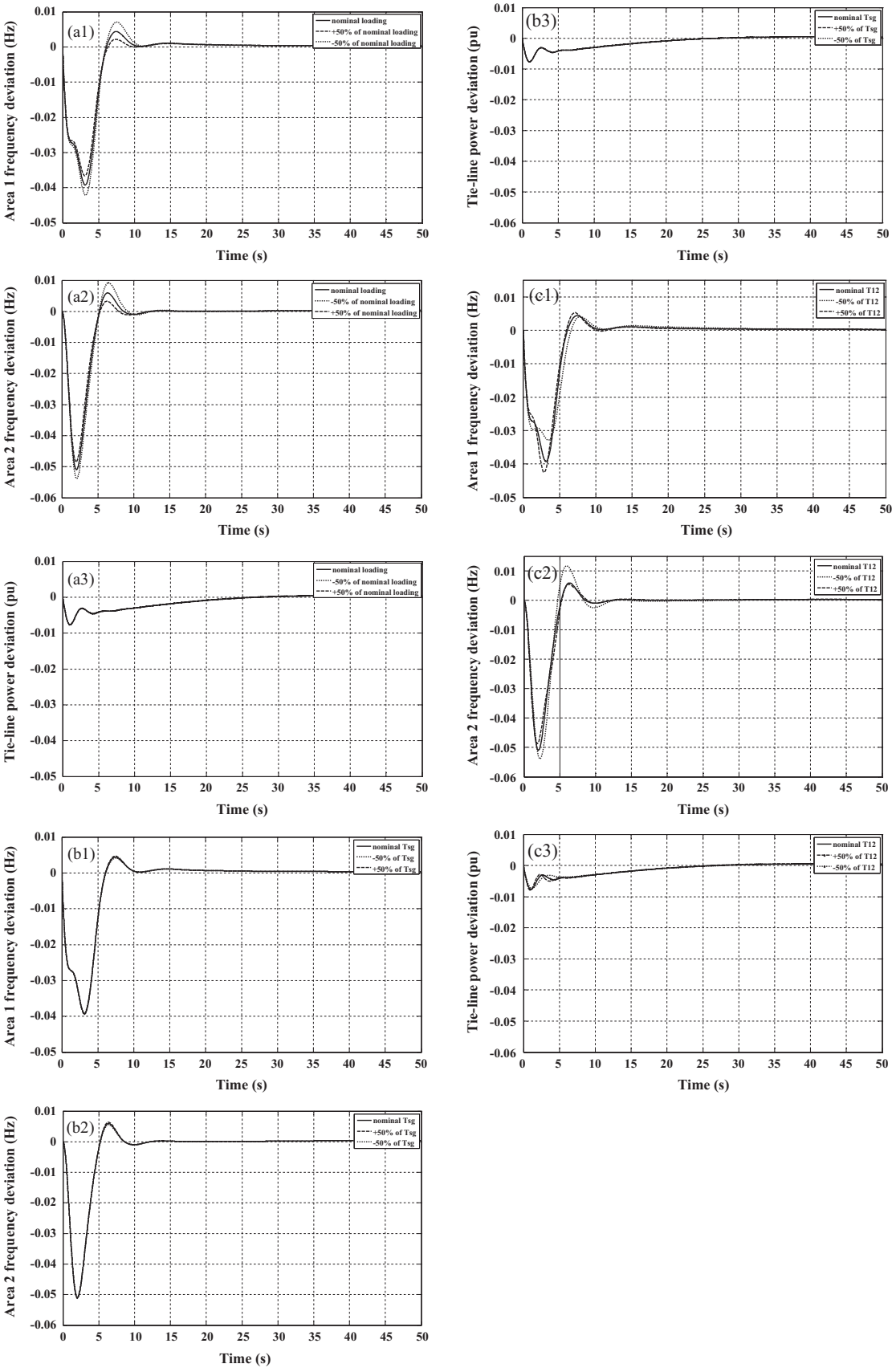

Fig. 7. Dynamic responses to the uncertainties in: (a) loading condition, (b) T_{sg}, and (c) T_{12}.

(T_S) with 5% criterion, system oscillatory modes and damping ratios (ζ) corresponding to the optimized controller are presented in Table 4. These stability measures are very important in evaluating the AGC dynamic performance. It is noteworthy to remark that since the applied disturbance is an increased load demand; the area frequency drops down at first with undershoot.

It can be seen from Fig. 4 that the integral controller can regulate the deviations to zero with difficulty. As it is obvious, even with the optimized integral gains, the area frequencies and the tie-line power oscillations persist for a long time. In this case, the AGC system can no longer suppress the frequency and tie-line power oscillations and drive back them to zero, effectively. It is clear from Fig. 4 that the proposed TCSC damping controller performs very effective in damping of area frequencies and tie-line power oscillations indeed in terms of decreased T_S, T_P, and M_p compared to those responses obtained by just AGC.

It is obvious from Table 4 that the M_p, T_P, and T_S of the dynamic responses obtained from TCSC–AGC coordination are significantly smaller than those of obtained from the just AGC case. In brief, outstanding stability improvement is obtained by employing the TCSC–AGC.

Simulation of the realistic power system for pulse load perturbation

In this case, a pulse load disturbance with period of 40 s and amplitude of 0.01 P.U. is applied in area 1. The obtained area frequencies and tie-line power oscillation responses are depicted in Fig. 5. It can be observed that by employing only AGC, the amplitude of the oscillations increases continuously which may lead to system instability, ultimately. Due to the advantages of the novel TCSC–AGC controller, the simulation results show that the oscillations are damped significantly and TCSC–AGC coordination provides a quite robust damping control for the load perturbation in pulse pattern.

Simulation of the realistic power system for sinusoidal load perturbation

The sinusoidal load perturbation is applied to evaluate the effectiveness of TCSC–AGC controller in area frequencies and tie-line power stabilization under contiguous load disturbance. The considered sinusoidal load perturbation is assumed as following [7], which is applied to the area 1:

$$\Delta P_{d1} = 0.03\sin(4.36t) + 0.05\sin(5.3t) - 0.1\sin(6t) \quad (17)$$

Fig. 6 illustrates the area 2 frequency and tie-line power deviations to the sinusoidal load perturbation. The simulations show that the responses are limited significantly by employing the TCSC–AGC controller. It should be noted that only the amplitude of oscillations with respect to this perturbation pattern is restricted, but it is not damped out. Because, the sinusoidal load perturbation takes place continuously in all the simulation time. However, TCSC–AGC controller provides superior stabilizing performance to the oscillations.

Table 6
Optimized parameters of advanced TCSC–AGC controller.

K_{l1}	K_{l2}	K_{TCSC}	T_{TCSC}	T_1	T_3	ITSE
0.1202	0.1800	0.1144	0.0599	0.5000	0.3108	0.0245

Sensitivity analysis against system loading condition and parametric uncertainties

In order to investigate the robustness of proposed TCSC–AGC controller to wide variation in the system loading condition and parameters, sensitivity analysis is carried out. The loading condition, governor time constant of thermal units T_{sg}, and the synchronizing coefficient T_{12} are varied in the range of ±50% from their nominal values, individually. The simulation results with these changed conditions for 0.01 P.U. SLP in area 1 are summarized in Table 5. The dynamic responses with aforementioned uncertainties are depicted in Fig. 7. From comparison of Table 5 with Table 4, also Fig. 7 with Fig. 4, one can be inferred that there is insignificant impact of the changes in the system loading condition and parameters on the obtained results in that the frequencies and tie-line power oscillations are suppressed as well. It can be observed from Table 5 that considering ±50% uncertainties in loading condition, T_{sg}, and T_{12} bring about negligible changes in value of ITSE index and other damping characteristics. Increase (or decrease) of ITSE index can be interpreted as decrease (or increase) of system damping performance. Thus, the sensitivity analysis reveals that proposed TCSC–AGC coordinated controller is quite robust; since, the optimized TCSC–AGC controller at the nominal loading condition with nominal parameters performs satisfactorily under the uncertainty scenarios. Thereby, the optimal parameters of the controller once set for nominal condition need not to be set again for ±50% variations in the system parameters and loading condition.

Simulation of the realistic power system with advanced TCSC damping controller

In order to obtain a more efficient TCSC-based damping controller than the basic, the structure of Fig. 8 is proposed where the two lead-lag blocks connected with T_1 to T_4 time constants supply the required phase lead characteristics to compensate the phase lag in the system. To reach this aim, the lead time constants (T_1, T_3) should be tuned above the given value of corresponding lag time constants (T_2, T_4) which here are considered 0.01s. The optimized parameters of advanced TCSC–AGC controller are shown in Table 6. It is clear that the value of obtained ITSE index with advanced TCSC–AGC controller (i.e. 0.0245) is smaller than that of obtained

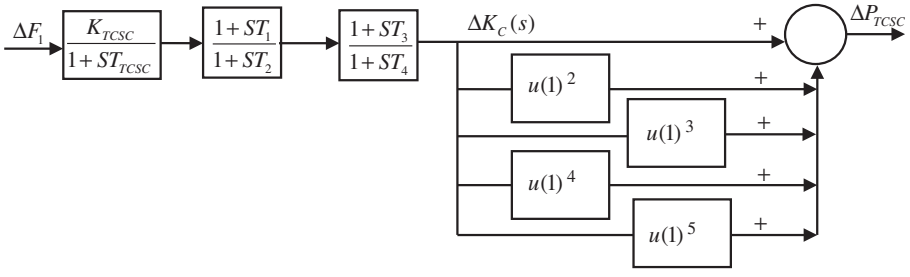

Fig. 8. Advanced structure for the TCSC based damping controller.

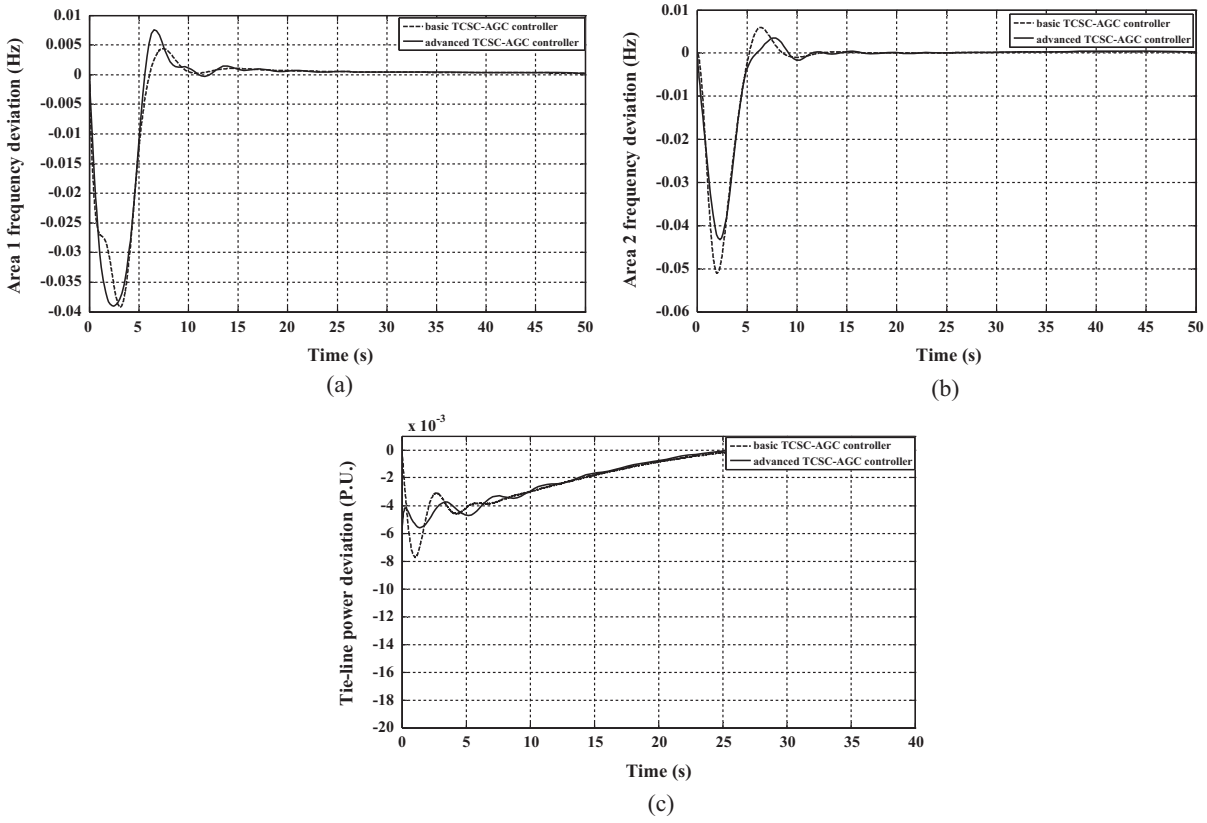

Fig. 9. Dynamic responses obtained by the proposed basic and advanced TCSC–AGC controllers: (a) area 1 frequency deviation Δf_1, (b) area 2 frequency deviation Δf_2, and (c) tie-line power deviation ΔP_{12}.

using the basic controller (0.0255 as depicted in Table 3). This indicates that proposed advanced controller is more effective than the basic scheme to suppress the oscillations. Fig. 9 shows the dynamic responses with application of this advanced TCSC structure in comparison with the basic TCSC model. It can be observed that the advanced controller can attain better results than the basic one, in general.

Conclusion

In this paper an effort has been made to enhance the dynamic stability of the power system by introducing a novel damping controller based on the TCSC in coordination with the AGC. The Taylor series expansion method has been used to model the TCSC-based damping controller. Basic and advanced structures for the damping controller have been presented. The dynamic performance of the novel TCSC–AGC coordinated controller has been verified on the realistic interconnected multi-source power system considering GRC and GDB nonlinearities. The effectiveness of TCSC–AGC controller in damping of the frequency and tie-line power oscillations has been compared with the case of just AGC. The time domain simulation results show that the TCSC–AGC controller yields greater dynamic performance in terms of reduced maximum peak, peak time, and settling time. Also, the robustness of the system equipped with the novel controller has been examined by sensitivity analyses for pulse load perturbation, sinusoidal load perturbation, and uncertainty scenarios in system loading condition and parameters. These analyses exhibit that the optimized TCSC–AGC is quite robust and performs satisfactorily under uncertainty conditions.

References

[1] Bhatt P, Roy R, Ghoshal S. GA/particle swarm intelligence based optimization of two specific varieties of controller devices applied to two-area multi-units automatic generation control. Int J Electr Power Energy Syst 2010;32:299–310.
[2] Joseph R, Das D, Patra A. Damping oscillations in tie-power and area frequencies in a thermal power system with SMES–TCPS combination. J Electr Syst 2011;7:71–80.
[3] Abraham RJ, Das D, Patra A. AGC study of a hydrothermal system with SMES and TCPS. Eur Trans Electr Power 2009;19:487–98.
[4] Rao CS, Nagaraju SS, Raju PS. Automatic generation control of TCPS based hydrothermal system under open market scenario: a fuzzy logic approach. Int J Electr Power Energy Syst 2009;31:315–22.
[5] Bhatt P, Ghoshal S, Roy R. Coordinated control of TCPS and SMES for frequency regulation of interconnected restructured power systems with dynamic participation from DFIG based wind farm. Renewable Energy 2012;40:40–50.
[6] Chidambaram I, Paramasivam B. Genetic algorithm based decentralized controller for load-frequency control of interconnected power systems with RFB considering TCPS in the tie-line. Int J Electron Eng Res 2009;1:299–312.
[7] Bhatt P, Roy R, Ghoshal S. Comparative performance evaluation of SMES–SMES, TCPS–SMES and SSSC–SMES controllers in automatic generation control for a two-area hydro–hydro system. Int J Electr Power Energy Syst 2011;33:1585–97.
[8] Parmar KPS, Majhi S, Kothari DP. LFC of an interconnected power system with thyristor controlled phase shifter in the tie line. Int J Comput Appl 2012;41.
[9] Subbaramaiah K. Comparison of performance of SSSC and TCPS in automatic generation control of hydrothermal system under deregulated scenario. Int J Electr Comput Eng (IJECE) 2011;1:21–30.
[10] Chidambaram I, Paramasivam B. Control performance standards based load-frequency controller considering redox flow batteries coordinate with interline power flow controller. J Power Sources 2012;219:292–304.
[11] Chidambaram I, Paramasivam B. Optimized load-frequency simulation in restructured power system with redox flow batteries and interline power flow controller. Int J Electr Power Energy Syst 2013;50:9–24.
[12] Meikandasivam S, Nema RK, Jain SK. Fine power flow control by split TCSC. Int J Electr Power Energy Syst 2013;45:519–29.
[13] Duong T, JianGang Y, Truong V. A new method for secured optimal power flow under normal and network contingencies via optimal location of TCSC. Int J Electr Power Energy Syst 2013;52:68–80.
[14] Padiyar KR. FACTS controllers in power transmission and distribution. New Age International; 2007.

[15] Song YH, Johns AT. Flexible ac transmission systems (FACTS). UK: Institution of Electrical Engineers; 1999.
[16] Shayeghi H, Shayanfar HA, Jalilzadeh S, Safari A. TCSC robust damping controller design based on particle swarm optimization for a multi-machine power system. Energy Convers Manage 2010;51:1873–82.
[17] Panda S. Differential evolutionary algorithm for TCSC-based controller design. Simul Model Pract Theory 2009;17:1618–34.
[18] Morsali J, Kazemzadeh R, Azizian MR. Coordinated design of MPSS and TCSC-based damping controller using PSO to enhance multi-machine power system stability. In: 21st Iranian conference on electrical engineering (ICEE); 2013. p. 1–6.
[19] Ali E, Abd-Elazim S. Coordinated design of PSSs and TCSC via bacterial swarm optimization algorithm in a multimachine power system. Int J Electr Power Energy Syst 2012;36:84–92.
[20] Shayeghi H, Safari A, Shayanfar H. PSS and TCSC damping controller coordinated design using PSO in multi-machine power system. Energy Convers Manage 2010;51:2930–7.
[21] Gozde H, Taplamacioglu MC. Automatic generation control application with craziness based particle swarm optimization in a thermal power system. Int J Electr Power Energy Syst 2011;33:8–16.
[22] Ganapathy S, Velusami S. MOEA based design of decentralized controllers for LFC of interconnected power systems with nonlinearities, AC–DC parallel tie-lines and SMES units. Energy Convers Manage 2010;51:873–80.
[23] Bevrani H, Hiyama T. Intelligent automatic generation control. CRC Press; 2011.
[24] Bevrani H. Robust power system frequency control. Springer; 2009.
[25] Challa KK, Rao PN. Analysis and design of controller for two area thermal-hydro-gas AGC system. In: Power electronics, drives and energy systems (PEDES) & 2010 Power India, 2010 Joint International Conference on: IEEE; 2010. p. 1–4.
[26] Ramakrishna K, Bhatti T. Automatic generation control of single area power system with multi-source power generation. Proc Instit Mech Eng, Part A: J Power Energy 2008;222:1–11.
[27] Ramakrishna K, Sharma P, Bhatti T. Automatic generation control of interconnected power system with diverse sources of power generation. Int J Eng, Sci Technol 2010;2:51–65.
[28] Parmar K, Majhi S, Kothari D. Load frequency control of a realistic power system with multi-source power generation. Int J Electr Power Energy Syst 2012;42:426–33.
[29] Mohanty B, Panda S, Hota P. Controller parameters tuning of differential evolution algorithm and its application to load frequency control of multi-source power system. Int J Electr Power Energy Syst 2014;54:77–85.
[30] Sahu RK, Panda S, Rout UK. DE optimized parallel 2-DOF PID controller for load frequency control of power system with governor dead-band nonlinearity. Int J Electr Power Energy Syst 2013;49:19–33.
[31] Kothari M, Satsangi P, Nanda J. Sampled-data automatic generation control of interconnected reheat thermal systems considering generation rate constraints. In: IEEE transactions on power apparatus and systems. PAS-100; 1981. p. 2334–42.
[32] Hingorani NG, Gyugyi L. Understanding FACTS; concepts and technology of flexible AC transmission systems. USA: IEEE Press; 2000.
[33] Miller TJE. Reactive power control in electric systems. USA: Wiley; 1982.
[34] Finney RL, Thomas GB, Weir MD. Calculus and analytic geometry. Addison-Wesley; 1992.
[35] Vijaya Chandrakala K, Balamurugan S, Sankaranarayanan K. Variable structure fuzzy gain scheduling based load frequency controller for multi source multi area hydro thermal system. Int J Electr Power Energy Syst 2013;53:375–81.
[36] Park J-B, Jeong Y-W, Shin J-R, Lee KY. An improved particle swarm optimization for nonconvex economic dispatch problems. IEEE Trans Power Syst 2010;25:156–66.